

# **Structural and electrical characterization of lead metaniobate thin films deposited by pulsed laser ablation**

F. CARDOSO, B.G. ALMEIDA, P. CALDELAS, J.A. MENDES, J. BARBOSA

*Departamento de Física, Universidade do Minho, Campus de Gualtar, 4710-057 Braga*

*Portugal*

## **Abstract**

Lead niobate thin films have been prepared by laser ablation, at different substrate temperatures ( $T_{\text{dep}}$ ) and with different oxygen pressures ( $p\text{O}_2$ ). For low deposition temperatures the films presented a rhombohedral- $\text{PbNb}_2\text{O}_6$  structural phase, with hysteresis cycles characteristic of a paraelectric. As  $T_{\text{dep}}$  increased the films started to develop an orthorhombic-  $\text{PbNb}_2\text{O}_6$  structure that appeared at  $400^\circ\text{C}$  and remained up to  $600^\circ\text{C}$ . For low  $p\text{O}_2$ , a mixture of this phase and a lead deficient phase was present in the films. Increasing the oxygen pressure the lead deficient phase was strongly reduced and the films presented only the ferroelectric orthorhombic-  $\text{PbNb}_2\text{O}_6$  structural phase.

RUNNING HEAD: Structure and electric characterization of lead niobate

## INTRODUCTION

Lead metaniobate ( $\text{PbNb}_2\text{O}_6$ ) is a good candidate for high temperature piezoelectric transducers due to its low mechanical quality factor  $Q$ , large anisotropy in the electromechanical coupling coefficient and high Curie temperature ( $570^\circ\text{C}$ ) [1-6]. At temperatures above  $1200^\circ\text{C}$  it has a tetragonal tungsten bronze structure. Upon cooling below  $1200^\circ\text{C}$  it transforms to a rhombohedral form that is paraelectric at room temperature. The rhombohedral form is not far from cubic ( $\alpha_{\text{rh}} = 93.9^\circ$ ) and has a perovskite like structure with alternate planes of  $\text{PbO}_3$  and (vacant-site) $\text{O}_3$ , in composition [7]. If the cooling through the  $1200^\circ\text{C}$ - $700^\circ\text{C}$  interval is fast, the tetragonal phase is retained down to  $570^\circ\text{C}$  where it changes to a ferroelectric orthorhombic metastable structure [5]. The orthorhombic lattice parameters are  $a=17.51\text{\AA}$ ,  $b=17.51\text{\AA}$  and  $c=7.73\text{\AA}$  [7]

In ceramic form, dense  $\text{PbNb}_2\text{O}_6$  is difficult to obtain by conventional techniques because of exaggerated grain growth due to the structural phase transformation from rhombohedral to tetragonal, during sintering [6]. In fact, when lead niobate is quenched from  $1200^\circ\text{C}$  it experiences severe cracking, limiting its practical applications. To obtain the ferroelectric orthorhombic phase at reasonable cooling rates, various dopants such as  $\text{ZrTiO}_4$  [5] and  $\text{Bi}_4\text{Ti}_3\text{O}_{12}$  [8] have been used to stabilize the ferroelectric phase.

Also, when  $\text{PbO}$  reacts with  $\text{Nb}_2\text{O}_5$ , with different molar ratios, lead niobate compounds having pyrochlore related structures are formed when the lead content is higher than that of niobium [9]. On the other hand, when the niobium content is higher, lead niobate compounds crystallize with tungsten bronze type structures [10].

In thin film form, using sputtering [11] or sol-gel techniques [12], the ferroelectric orthorhombic lead niobate phase can be stabilized at lower temperatures ( $450$ - $900^\circ\text{C}$  [11,12]) as compared to ceramics. However, the stabilization of the ferroelectric orthorhombic phase is difficult due to the formation of non-ferroelectric phases during deposition. In order to

address this problem, lead metaniobate thin films have been prepared at different substrate temperatures and with different oxygen pressures, during deposition.

## **EXPERIMENTAL**

The films were prepared by pulsed laser ablation on Pt/TiO<sub>2</sub>/SiO<sub>2</sub>/(001)Si substrates. The depositions were done with a KrF excimer laser with wavelength  $\lambda=248\text{nm}$ , at a fluence of  $1.5\text{J}/\text{cm}^2$ . The target was composed of a compressed lead niobate powder, sintered at  $1200^\circ\text{C}$  during one hour. The X-ray diffraction spectrum measured on the target showed that it was polycrystalline and composed by PbNb<sub>2</sub>O<sub>6</sub> with a rhombohedral structure. A residual Pb<sub>3</sub>Nb<sub>4</sub>O<sub>13</sub> phase with a cubic pyrochlore structure was also observed. This phase has an excess of lead in its composition, as compared to PbNb<sub>2</sub>O<sub>6</sub>.

The oxygen pressure during film preparation ( $p\text{O}_2$ ) was in the range  $10^{-3}$ - $2\times 10^{-2}$  mbar and the substrate temperature varied from room temperature to  $600^\circ\text{C}$ . The distance from the target to the substrate ( $d_{\text{ST}}$ ) was 2.3cm. The structural studies were performed by X-ray diffraction (XRD) and were carried out with a Philips PW-1710 diffractometer using Cu K $\alpha$  radiation. The surface of the films was examined by scanning electron microscopy (SEM). The polarization versus electric field hysteresis loops were measured at room temperature, using a Sawyer-Tower circuit.

## **RESULTS AND DISCUSSION**

Figure 1 show SEM micrographs obtained on samples deposited a) at  $500^\circ\text{C}$  with  $p\text{O}_2=8\times 10^{-3}$  mbar and b) at  $600^\circ\text{C}$  with  $p\text{O}_2=2\times 10^{-2}$  mbar.

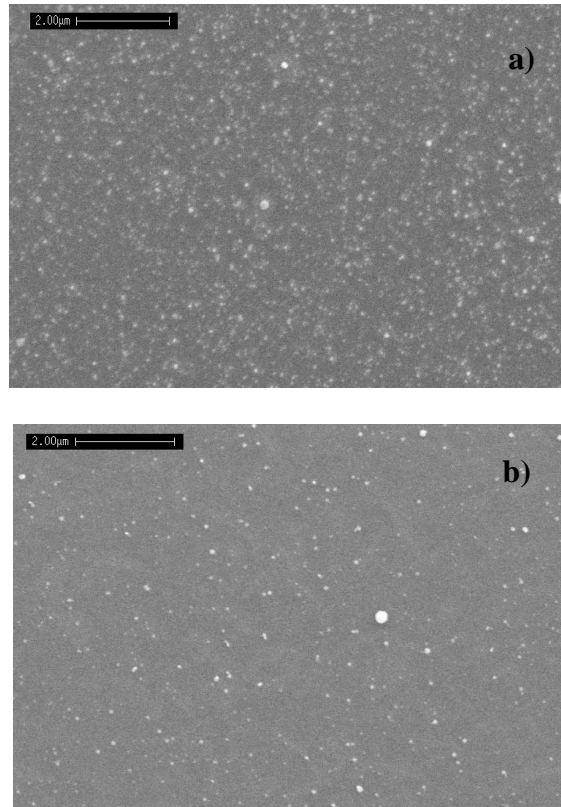


FIGURE 1: SEM micrographs of the surface of the films deposited with a)  $T_{\text{dep}}=500^{\circ}\text{C}$  and  $p\text{O}_2=8\times 10^{-3}\text{mbar}$ , and b)  $T_{\text{dep}}=600^{\circ}\text{C}$  and  $p\text{O}_2=2\times 10^{-2}\text{mbar}$ .

The films present a granular surface with average grain sizes, determined from the SEM micrographs, of  $588\text{ \AA}$  and  $507\text{ \AA}$ , respectively. For higher oxygen pressure we observe a less grainy surface and the films are denser. Inherent to the laser ablation technique is the appearance of small droplets ( $\sim 0.5 - 2\text{ }\mu\text{m}$ ) on the films surface. In our samples, the surface shows a low density of these droplets.

Figures 2a)-2c) show the X-ray diffraction spectra measured on films deposited at  $400^{\circ}\text{C}$ ,  $500^{\circ}\text{C}$  and  $600^{\circ}\text{C}$ , with lower oxygen pressures ( $4-8\times 10^{-3}\text{mbar}$ ). Figures 2d)-2g) show the X-ray diffraction spectra measured on films deposited at  $200^{\circ}\text{C}$ ,  $400^{\circ}\text{C}$ ,  $500^{\circ}\text{C}$  and  $600^{\circ}\text{C}$ , with higher oxygen pressures ( $1-2\times 10^{-2}\text{mbar}$ ). Figure 3 show and enlargement of the X-ray diffraction spectra of figure 2, in the  $2\theta$  angle range  $20^{\circ}-34^{\circ}$ .

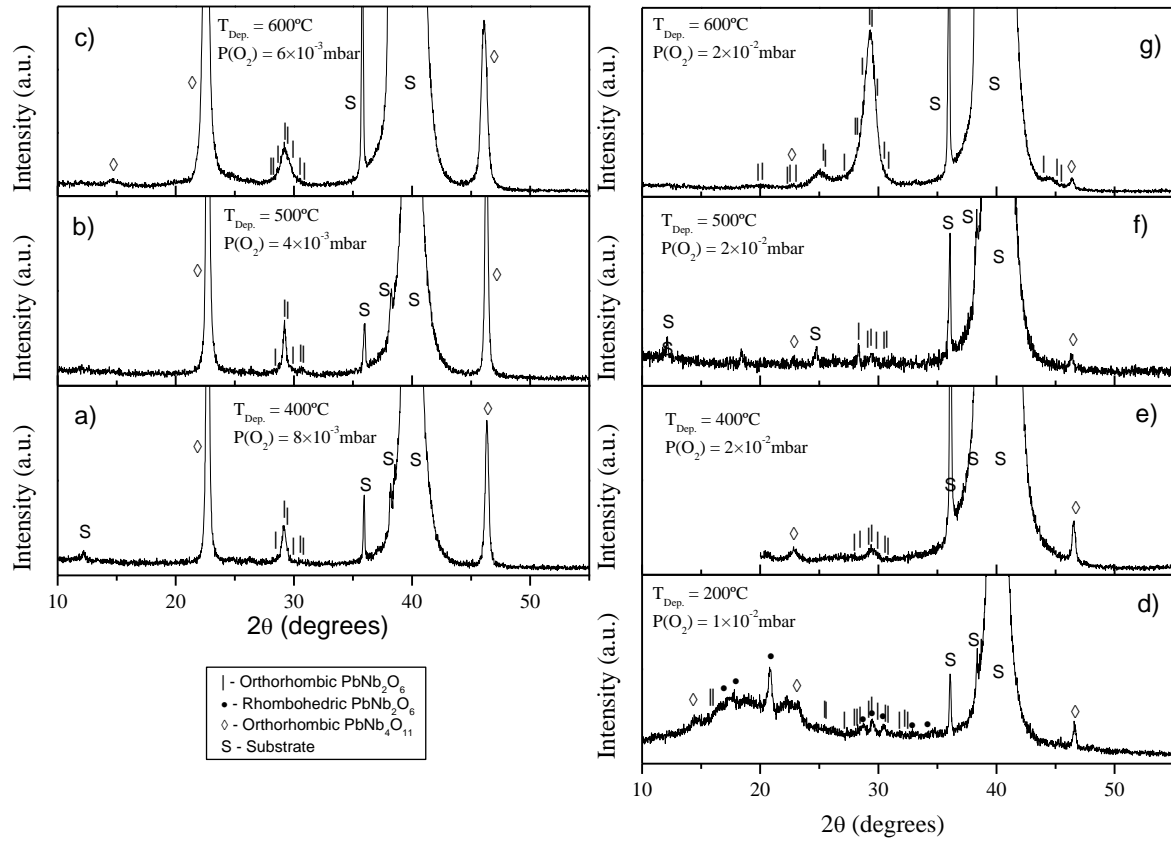


FIGURE 2: X-ray diffraction spectra measured on the samples deposited with substrate temperature in the range 400°C-600°C, and oxygen pressures a)-c)  $4\text{-}8\times 10^{-3}$  mbar and d)-g)  $1\text{-}2\times 10^{-2}$  mbar.

The vertical lines indicate the peak positions of the lead niobate orthorhombic- $\text{PbNb}_2\text{O}_6$  phase obtained in bulk samples. Open lozenges indicate the corresponding peak positions of a lead deficient  $\text{PbNb}_4\text{O}_{11}$  phase with orthorhombic structure, which is also present in the films. Figures 2 and 3 indicate that their composition is a mixture of orthorhombic- $\text{PbNb}_2\text{O}_6$  or rhombohedral- $\text{PbNb}_2\text{O}_6$  with the lead deficient  $\text{PbNb}_4\text{O}_{11}$  phase. The proportions of the different phases vary with deposition temperature and oxygen pressure.

For low deposition temperatures ( $T_{\text{dep}}\sim 200^\circ\text{C}$ ) the films present a polycrystalline rhombohedral- $\text{PbNb}_2\text{O}_6$  structural phase (fig. 2d). In figure 3, the black circles mark the peaks corresponding to the bulk rhombohedral phase that exist in this angle interval. They

occur at  $2\theta$  angles  $21.0^\circ$ ,  $28.7^\circ$ ,  $29.5^\circ$  and  $30.5^\circ$ , and correspond to the lattice planes (021), (113), (300), and (122).

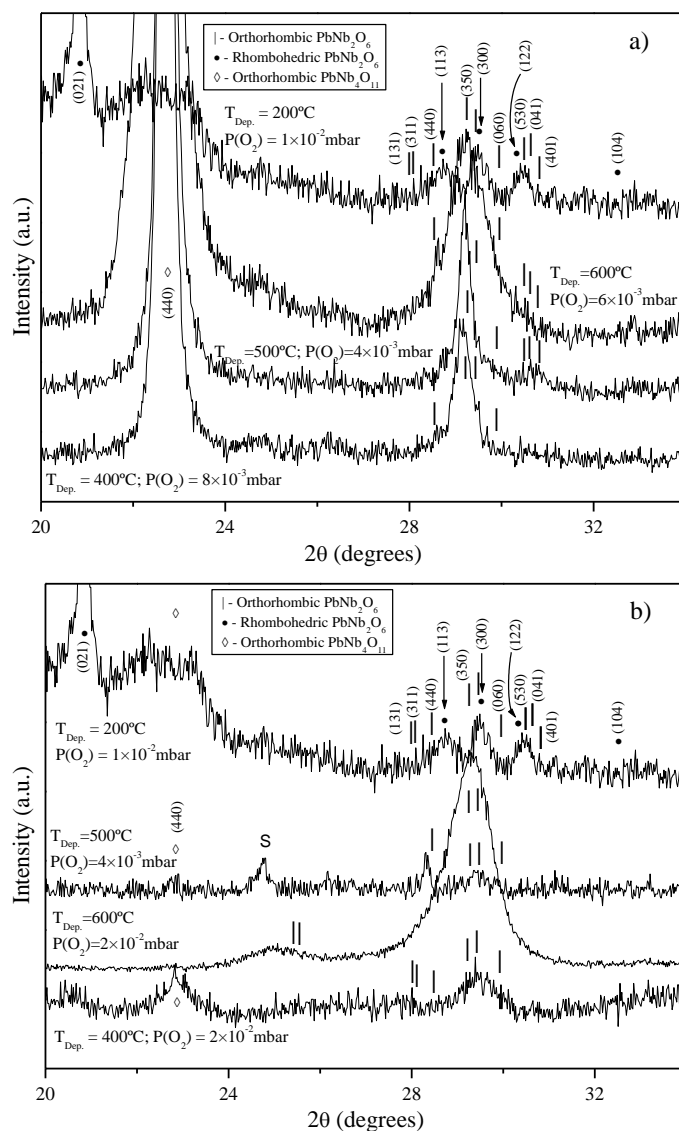


FIGURE 3: X-ray diffraction peaks for the films of figure 2 deposited with a) lower oxygen pressure and b) higher oxygen pressure, plotted on an expanded scale.

As  $T_{\text{dep}}$  increases above  $400^\circ\text{C}$  the films start to develop an orthorhombic- $\text{PbNb}_2\text{O}_6$  structure that remains up to  $600^\circ\text{C}$ . This is revealed by the appearance of peaks, located between the rhombohedral (113) and (300) directions, at a  $2\theta$  position between  $28.6^\circ$  and  $30.1^\circ$ , and of three peaks located between  $2\theta \sim 42^\circ$  and  $45^\circ$  which are observed in the films deposited at  $600^\circ\text{C}$  and correspond to the planes [660], [750] and [371]. On samples grown at

400°C and 500°C, with low oxygen pressure ( $p_{O_2} \leq 8 \times 10^{-3}$  mbar), the peak at  $2\theta = 29.2^\circ$  matches the orthorhombic-PbNb<sub>2</sub>O<sub>6</sub> (350) lattice direction and its relative intensity indicate that the films have a (350) preferential orientation. For films grown at 600°C with lower oxygen pressure the shape of the peak occurring near 29.2° indicates that it is a superposition of multiple peaks. A fit with multiple gaussian functions overlapping each other, gave the positions 29.2°, 29.5° and 30.0°, which are consistent with the bulk orthorhombic-PbNb<sub>2</sub>O<sub>6</sub> peak positions of the (113), (350) and (300) directions shown in figure 3a). In samples grown with higher oxygen pressures, these three peaks are always present indicating a more polycrystalline structure, and the absence of a clear preferential growth direction. The X-ray diffraction coherence length for the orthorhombic-PbNb<sub>2</sub>O<sub>6</sub> phase was determined from the (350) peak by using the Scherrer equation [13]. The values obtained on the deposited films were used as a measure of their grains size and were found to be in the range 200-650 Å, as shown in figure 4. They are consistent with values determined by direct observation in the SEM.

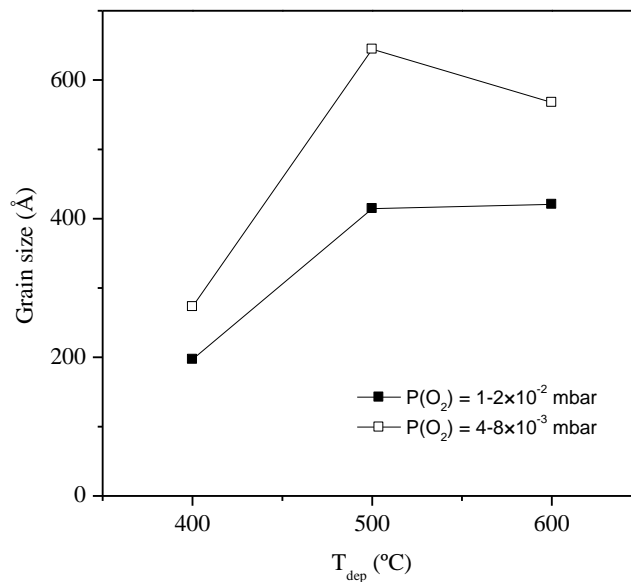


FIGURE 4: Grain size of the orthorhombic lead niobate PbNb<sub>2</sub>O<sub>6</sub> phase, determined from the (350) peak width.

The average grain size increases with increasing deposition temperature and is smaller on samples deposited with higher oxygen pressures, due to the more polycrystalline structure of these films.

Figure 5 shows the relative intensity between the (350) peak of the orthorhombic- $\text{PbNb}_2\text{O}_6$  phase and the (440) peak of the lead deficient  $\text{PbNb}_4\text{O}_{11}$  phase.

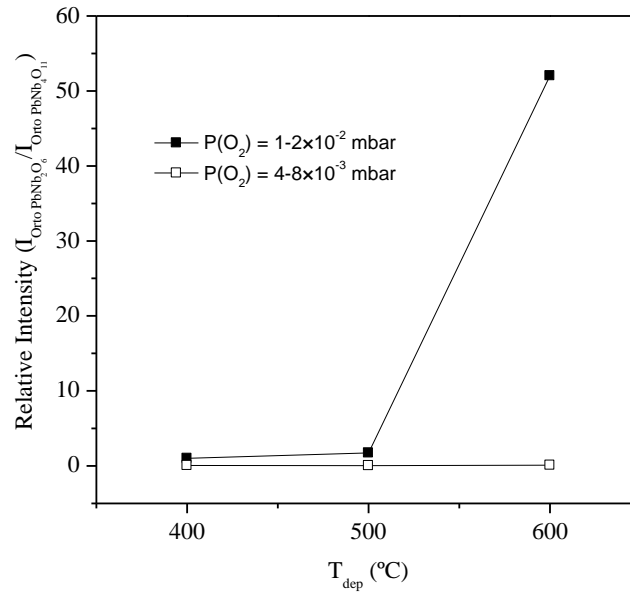


FIGURE 5: Relative intensity of the (350) peak of the orthorhombic  $\text{PbNb}_2\text{O}_6$ , and (440) of the orthorhombic  $\text{PbNb}_4\text{O}_{11}$ , as a function of temperature.

For lower oxygen pressures, the relative intensity rises from 0.06 at  $T_{\text{dep}}=400^\circ\text{C}$  to 0.1 for  $T_{\text{dep}}=600^\circ\text{C}$  indicating that the lead deficient phase in fact dominates the composition of these films. On the other hand, by increasing the oxygen pressure, the relative intensity strongly increases (from 1 at  $T_{\text{dep}}=400^\circ\text{C}$  to 52 at  $T_{\text{dep}}=600^\circ\text{C}$ ), so that mainly the orthorhombic- $\text{PbNb}_2\text{O}_6$  form composes the films and only a residual lead deficient phase is observed in the X-ray diffraction spectra (figure 2). Thus, the increase of the oxygen pressure during deposition favors the formation of the orthorhombic- $\text{PbNb}_2\text{O}_6$  phase, as compared to the lead deficient  $\text{PbNb}_4\text{O}_{11}$ .

In the pressure range that was used during film deposition ( $4 \times 10^{-3}$  mbar to  $2 \times 10^{-2}$  mbar) we are in a regime where the plume created when the laser interacts with the target has



a length ( $\sim 3$  cm for  $2 \times 10^{-2}$  mbar [14-16]) that is of the order, or higher than, the distance from the target to the substrate ( $d_{ST}=2.3$ cm). So the incident flux on the substrate is not thermalized and re-sputtering should be approximately the same in all the pressure range used.

Assuming that the plume, is mainly formed by atomic species (Pb and Nb) and considering a simple scattering model based on hard-spheres [14], it is possible to estimate the mean free path ( $\lambda$ ) of Pb or Nb atoms in  $O_2$  according to the expression:

$$\lambda = \frac{k_B T}{\pi P d^2} \quad (1)$$

where  $k_B$  is the Boltzmann constant,  $T$  is the temperature of the background  $O_2$  gas atmosphere,  $P$  is the gas pressure, and  $d = r_i + r_{O_2}$  is the impact parameter ( $r_i$  and  $r_{O_2}$  being the radii of the species  $i$  (Pb or Nb) and  $O_2$ ). To calculate the mean free paths, the values of the atomic radii of Pb, Nb, and  $O_2$  that were used were [14,17]:  $r_{O_2} = 1.8 \text{ \AA}$ ,  $r_{Pb} = 1.54 \text{ \AA}$ , and  $r_{Nb} = 1.98 \text{ \AA}$ . Their atomic masses are [17]  $m_{Pb} = 207$  and  $m_{Nb} = 93$ .

In the pressure region  $4-8 \times 10^{-3}$  mbar, the mean free paths of Nb and Pb ( $\lambda_{Nb} = 2.1$ cm and  $\lambda_{Pb} = 1.8$ cm for  $T_{dep} = 400^\circ\text{C}$ , and  $\lambda_{Nb} = 3.2$ cm and  $\lambda_{Pb} = 2.6$ cm for  $T_{dep} = 600^\circ\text{C}$ ) are of the order, or higher, than the distance from the target to substrate ( $d_{ST} = 2.3$ cm). Then, the higher mean free path of Nb and the higher volatility of lead favor the formation of the lead deficient  $PbNb_4O_{11}$  phase at lower oxygen pressures.

On the other hand, in the pressure region  $1-2 \times 10^{-2}$  mbar the mean free paths of Pb and Nb ( $\lambda_{Nb} = 0.8$ cm and  $\lambda_{Pb} = 0.7$ cm for  $T_{dep} = 400^\circ\text{C}$ , and  $\lambda_{Nb} = 1.2$ cm and  $\lambda_{Pb} = 1.0$ cm for  $T_{dep} = 600^\circ\text{C}$ ) become much shorter than the distance from the target to the substrate. Then, the number of collisions that Nb and Pb atoms experience until they reach the substrate is high and the dominant effect that determines the relative amount of Pb and Nb in the deposited films is the masses [14]. Since  $m_{Pb} > m_{Nb}$ , the broadening of the angular distribution of Pb atoms arriving at the substrate is smaller than that of Nb. So, the relative number of atoms of

Pb traveling along the normal to the target will be higher. This then leads to a reduction of the lead deficiency in the films deposited at higher oxygen pressures, and to the stabilization of the orthorhombic-PbNb<sub>2</sub>O<sub>6</sub> phase as shown in figure 5.

Figure 6 shows the polarization hysteresis cycles measured on the samples deposited with a)  $T_{\text{dep}}=200^{\circ}\text{C}$  and  $p\text{O}_2=8\times 10^{-3}\text{mbar}$  and b)  $T_{\text{dep}}=600^{\circ}\text{C}$  and  $p\text{O}_2=2\times 10^{-2}\text{mbar}$ .

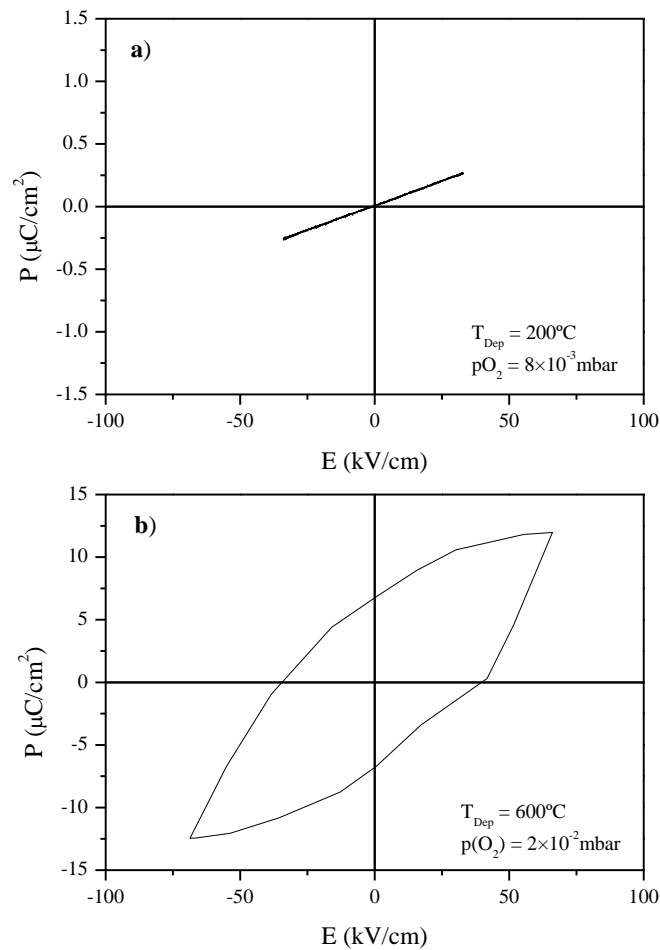


FIGURE 6. Polarization as a function of applied electric field, measured on the samples deposited with a)  $T_{\text{dep}}=200^{\circ}\text{C}$  and  $p\text{O}_2=8\times 10^{-3}\text{mbar}$  and b)  $T_{\text{dep}}=600^{\circ}\text{C}$  and  $p\text{O}_2=2\times 10^{-2}\text{mbar}$ .

For films deposited at lower temperature the polarization hysteresis loops present a linear dependence (fig. 6a), consistent with the paraelectric behaviour of the rhombohedral phase. On the other hand for the samples deposited at higher oxygen pressure and substrate temperature the cycles show a tendency towards saturation, as shown in figure 6b) for

$T_{\text{dep}}=600^{\circ}\text{C}$ . Similar unsaturated loops have been observed in bulk lead metaniobate ceramics [4,6,7], and in thin films [11,12]. In the case of figure 6b) the remanent polarization ( $P_r$ ) is  $6.7\mu\text{C}/\text{cm}^2$  and the coercivity  $E_c$  is  $34\text{kV}/\text{cm}$ . The value of  $P_r$  is lower than the remanent polarization obtained on sol-gel films ( $12.3\mu\text{C}/\text{cm}^2$ ) [12], and the polarization value is also lower than the  $15\mu\text{C}/\text{cm}^2$  obtained at  $500\text{kV}/\text{cm}$  on lead niobate films deposited by sputtering and then annealed by pulsed thermal processing [11]. This is due to the residual lead deficient  $\text{PbNb}_4\text{O}_{11}$  phase still present on the films deposited at higher oxygen pressures ( $p\text{O}_2=2\times 10^{-2}$  mbar) and substrate temperatures ( $T_{\text{dep}}=600^{\circ}\text{C}$ ), as show in the X-ray diffraction spectrum of figure 2g).

## CONCLUSIONS

Lead niobate thin films have been prepared by pulsed laser ablation at different oxygen pressures and substrate temperatures. For low oxygen pressures ( $p\text{O}_2\leq 8\times 10^{-3}$  mbar) they present an orthorhombic- $\text{PbNb}_2\text{O}_6$  structure mixed with a lead deficient phase with  $\text{PbNb}_4\text{O}_{11}$  stoichiometry. By increasing the substrate temperature and oxygen pressure the lead deficient phase was strongly reduced so that for  $T_{\text{dep}}=600^{\circ}\text{C}$  and  $p\text{O}_2=2\times 10^{-2}$  mbar the orthorhombic- $\text{PbNb}_2\text{O}_6$  phase dominated the films composition. Hysteresis cycles measured on these films presented ferroelectric hysteresis loops that do not show saturation, as already observed in bulk lead metaniobate ceramics and thin films.

## References

- [1] - Ray S., Gunther E., and Ritzhaupt-Kleissl H.J.: Manufacturing and characterization of piezoceramic lead metaniobate  $\text{PbNb}_2\text{O}_6$ . J. Mater. Sci. Vol. **35**, 6221 (2000)
- [2] - Eyraud P., Eyraud L., Gonnard P., Noterman D., and Troccaz M.: Electromechanical properties of  $\text{PbNb}_2\text{O}_6$  and  $\text{PbTiO}_3$  modified ceramics elaborated by a coprecipitation

process. *Proceedings of the Sixth IEEE International Symposium on Applications of Ferroelectrics*, New York: IEEE (1986)

[3] - Allahverdi M., Hall A., Brennan R., Ebrahimi M.E., Marandian Hagh N., and Safari A.: An overview of rapidly prototyped piezoelectric actuators and grain-oriented ceramics. *J. Electroceram.* **8**, 129 (2002)

[4] - Goodman G.: Ferroelectric properties of lead metaniobate. *J. Am. Ceram. Soc.* **36**, 368 (1953)

[5] - Moulson A.J., and Herbert J.M.: *Electroceramics*. London: Chapman and Hall (1990)

[6] - Sung Lee H., and Kimura T.: Effects of microstructure on the dielectric and piezoelectric properties of lead metaniobate. *J. Am. Ceram. Soc.* **81**, 3228 (1998)

[7] - Herbert J.M.: *Ferroelectric transducers and sensors*. London: Gordon and Breach, (1985)

[8] – Subbarao E.C. and Hrizo J.: *J. Am. Ceram. Soc.* **45**, 528 (1962)

[9] - Sreedhar K. and Mitra A.: Formation and transformation of cubic lead niobate pyrochlore solid solutions. *J. Am. Ceram. Soc.* **82**, 1070 (1999)

[10] - Brusset H., Mahé R., and Aung Kyi U.: Etude de niobates divalents binaires et ternaires a l'état solide. *Mat. Res. Bull.* **7**, 1061 (1972)

[11] - Vasant Kumar C.V.R., Sayer M., and Pascual R.: Ferroelectric lead niobate films by pulsed thermal processing. *Appl. Phys. Lett.* **60**, 2207 (1992)

[12] - Xue J.M., Ezhilvalavan S., Gao X.S., and Wang J.: Strontium titanate doped lead metaniobate ferroelectric thin films. *Appl. Phys. Lett.* **81**, 877 (2002)

[13] - Cullity B.D.: *Elements of X-Ray Diffraction*. Reading MA: Addison-Wesley, (1978)

[14] - Gonzalo J., Gomez San Roman R., Perrière J., Afonso C.N., Perez Casero R.: Pressure effects during pulsed-laser deposition of barium titanate thin films. *Appl. Phys. A* **66**, 487 (1998)

- [15] Kools, J.C.S.: Monte Carlo simulations of the transport of laser-ablated atoms in a diluted gas. *J. Appl. Phys.* **74**, 8401 (1993)
- [16] Geohegan, D.B.: Fast intensified-CCD photography of  $\text{YBa}_2\text{Cu}_3\text{O}_{7-x}$  laser ablation in vacuum and ambient oxygen. *Appl. Phys. Lett.* **60**, 2732 (1992).
- [17] - CRC Handbook of chemistry and physics 66<sup>th</sup> edition, R.C. Weast (Editor), Crc Press Inc (1985)